

# INFLIGHT INTERSENSOR RADIOMETRIC CALIBRATION USING THE REFLECTANCE-BASED METHOD FOR LANDSAT-TYPE SENSORS

**K. Thome, J. McCorkel, J. Czaplá-Myers**  
Remote Sensing Group, College of Optical Sciences  
University of Arizona  
Tucson, AZ 85721  
[kthome@email.arizona.edu](mailto:kthome@email.arizona.edu)  
[mccorkel@email.arizona.edu](mailto:mccorkel@email.arizona.edu)  
[j.czapla-myers@optics.arizona.edu](mailto:j.czapla-myers@optics.arizona.edu)

## ABSTRACT

Improvements in the protocols and approaches used for the inflight radiometric calibration and validation of imaging sensors using the reflectance-based method has led to the feasibility of this method for the intercomparison of multiple sensors. The philosophy presented here is different than the typical cross-calibration techniques used successfully since the 1980s in that it does not require near simultaneous views of the ground. The concept is similar to the use of spherical integrating sources as a calibration standard in multiple laboratories for multiple sensors. The maintenance of traceability of these sources to a set of specified standards allows sensors calibrated in the same way to agree within the uncertainties of the methods. Extending the idea of a calibration source to that of a ground-reference target readily shows how these concepts can be used inflight. Results using ASTER, Landsat-5 TM, Landsat-7 ETM+, and ALI illustrates that the method can be applied with precision approaching 1% (one standard deviation) in many spectral bands. The method relies on selecting data sets based on specific atmospheric and surface conditions and scaling data sets based on band-to-band correlations. Results are not limited to a single site and results from one sensor can be compared to those of another sensor without the need for coincident acquisitions. Disagreements between sensors in excess of 1.4% would be indicative of possible biases between the sensors.

## INTRODUCTION

The increase in the number and design of remote sensing systems over the past 20 years has led to an increased interest in comparing data from multiple sensors. The basis for data intercomparison and synergy is related to the well-known phrase, “the whole is greater than the sum of all its parts.” One example of a sensor suite exceeding the sum of its parts is the Terra and Landsat-7 platforms (Kaufman et al., 1998, Goward et al., 2001). The Advanced Spaceborne Thermal Emission and Reflection and Radiometer (ASTER), Multi-angle Imaging Spectroradiometer (MISR) and Moderate Resolution Imaging Spectroradiometer (MODIS) are three imaging sensors on the Terra platform with several common bands. Their varying resolutions and differences in spectral bands is the driving force behind the synergistic use of the data from Terra sensors. The goal of synergy between sensors was also the impetus for launching the Landsat-7 platform that has the Enhanced Thematic Mapper Plus (ETM+) sensor in an orbit that was approximately 30 minutes prior to Terra.

Critical to summing the parts from multiple sensors is that they agree radiometrically both in an absolute and a relative sense.(Butler and Barnes, 1998, Thome et al., 1997) This is not just true for these sensors but characterization and validation are crucial to all Earth Science Enterprise sensors. Such radiometric agreement should be feasible based solely on the prelaunch calibration of each individual sensor using accurate and traceable calibration approaches. Unfortunately, national standards can vary from country to country and the rigors of the launch process can impact sensors in different fashions. It thus becomes necessary to develop techniques for the calibration of sensors when they are on orbit and these calibration approaches should also include cross-calibration methods.

Typical methods for calibration and validation after launch involve either in-situ based measurements or model-based predictions (Slater et al., 1996) The model-based methods such as relying on atmospheric scattering or invariant surfaces provide high-precision data with high temporal sampling.(Kaufman and Holben, 1993; Vermote and Kaufman, 1992; Vermote et al., 1992; Cabot et al., 1999) Such data are excellent for analyzing trends in the radiometric

calibration of a sensor, but not necessarily sufficient from an absolute radiometric accuracy. Such approaches can be used for cross-calibration of similar instruments and have been used successfully for the calibration of the AVHRR and MODIS series of sensors. Use of these approaches for cross-calibration require simultaneous or near simultaneous views of the source or assumptions that the model-based predictions are stable in time. The results in both cases are improved if there is temporal overlap of the sensors being calibrated.

The above approaches are primarily used to determine the stability of a sensor and the precision of this stability characterization allows biases between sensors to be determined. Methods that emphasize accuracy with traceability to national standards allow cross-comparisons between sensors that do not overlap in time. Such approaches typically rely on in-situ measurements. Of course, the fact that they require in-situ data increases the cost of implementing them, both in terms of personnel time as well as the cost of deploying the equipment needed to collect the data. The Remote Sensing Group (RSG) at the University of Arizona has used one of these in-situ approaches, the reflectance-based approach, since the 1980s (Slater et al., 1987; Thome et al., 1993; Thome, 2001; Thome et al., 2004). Recent results show that the RSG produces results with precision that is approaching 2% in some bands (Thome et al., 2005a).

It is the improved precision of the reflectance-based approach and vicarious approaches in general that makes it possible to use these methods in the same fashion as preflight, laboratory calibrations to allow intercomparisons of sensors. Past work has shown that the method works well for determining differences between sensors that are near in time to each other (Thome et al., 2006). That work showed that changes in the radiometric calibration coefficients for ASTER improved the radiometric compatibility of the VNIR bands to other sensors but still led to significantly large differences between ASTER, ETM+, MISR, and MODIS in the green bands of these sensors. The precision of the absolute comparisons was better than 2% if care was taken to collect a consistent basis set of data for each in situ collection.

The current work demonstrates that the expected limit to the accuracy of cross comparisons using the reflectance-based method approaches 1.4% relative to the reflectance-based method. The sensors used here are limited to those with moderate resolutions from 15 to 30 m resolution but do not have coincidence in time. Analysis of the results indicates that this precision can be improved through additional field instrument characterization, higher frequency of collections, and separation of results by test site and users. The power of such a method should be clear when considering the lifetime records of Landsat. The goal is to continue these data records through the Landsat Data Continuity Mission. The current precision of vicarious methods should allow for a consistent data record across any gaps in sensors. The paper begins with a brief description of the reflectance-based approach as it applies to this work and the sensors considered. The intercomparison between sensors with coincident-date overpasses are presented followed by an analysis approach between the Landsat-5 and Landsat-7 sensors. The results are discussed in the context of probable improvements to the method to reduce uncertainties.

## **REFLECTANCE-BASED APPROACH**

The reflectance-based method uses ground-based measurements to characterize the surface of a test site and the atmosphere over that test site. The results of these characterizations are inputs to a radiative transfer code to predict at-sensor radiance. The approach has been used for a wide range of spatial resolutions at sites ranging in size from 100 m in size to over 30 km. (Thome et al., 2004, Thome et al., 2005b). The work shown here relies on data collected at the Railroad Valley Playa test site in Nevada and Ivanpah Playa in California. Details of the reflectance-based approach and both sites can be found in other sources, so only a brief overview is given here (Thome et al., 2004).

### **Test Sites**

The Railroad Valley test site is in central Nevada and has an overall size approximately 15 km by 15 km. The playa's 1.5 km elevation, location in a region with typically clear weather, low aerosol loading, and high surface reflectance makes it a good site for the reflectance-based approach. Typical atmospheric conditions at the site include an average aerosol optical depth at 550 nm of 0.060 (Thome et al., 2005a). The reflectance of the playa is generally greater than 0.3 and relatively flat spectrally except for the blue portion of the spectrum and an absorption feature in the shortwave infrared. Ground-based measurements of the directional reflectance characteristics of the playa show it to be nearly lambertian out to view angles of 30 degrees for incident solar zenith angles seen for overpasses of Terra and Landsat.

The Ivanpah Playa test site has similar reflectance characteristics but is in general brighter than Railroad Valley

Playa. Ivanpah Playa is significantly smaller than Railroad Valley Playa with a width of approximately 3 km and length of 5 km. The surface is much harder and is susceptible to standing water in the winter and after heavy summer rains. The elevation of 0.8 km makes atmospheric effects more important and the site has an average aerosol optical depth at 550 nm of 0.084 (Thome et al., 2005a). The Ivanpah site is closer to the RSG laboratory and as such has seen more frequent use than the Railroad Valley site.

### Sensor Overview

Four sensors are used in this work, the Advanced Land Imager (ALI), ASTER, ETM+, and Landsat-5 Thematic Mapper. All four have similar spatial resolution with similar spectral bands in the reflective portion of the spectrum. ALI has been designed to provide imagery with the same aspects of Landsat 7 ETM+ such as spatial resolution, swath width, spectral bands, orbit, and overpass time. Differences in ALI relative to ETM+ include the addition of three bands, panchromatic resolution improvement, and a higher 12-bit quantization (Lencioni et al., 1999). One fundamental difference between ALI and previous Landsat instruments is that it is a pushbroom system rather than a whiskbroom. Another distinct improvement of ALI is that the more technologically advanced design has about one-fourth the mass, one-fifth the power consumption, and about one-third the volume of Landsat 7 (Lencioni et al., 1999). However, ALI did not perform as required for stray light suppression (Robicaud et al., 2003).

ASTER, which is on the Terra platform, has a 60-km swath width with 14 total bands in the visible and near infrared (VNIR), shortwave infrared (SWIR), and thermal infrared (TIR) (Yamaguchi et al., 1998). The spatial resolution of the three VNIR bands is 15 m and that of the six SWIR bands is 30 m. The VNIR and SWIR sensors are pushbroom systems.

ETM+ and TM are nearly identical copies of each other. The sensors rely on a whiskbroom scanning approach to allow for the relatively large 185-km swath width. A warm focal plane is used for the four 30-m VNIR bands, and, in the case of ETM+, the 15-m panchromatic band. A cold focal plane is used for the two SWIR bands and also for the single TIR band. The TIR band has 120-m spatial resolution for TM and 60-m resolution for ETM+.

The spectral bands for each sensor are listed in Table 1. Reference is made throughout the paper to the band numbers for each of the sensors. The table shows that many of the bands are similar but with distinct differences. The differences between bands also extend to the bandwidths and these play a role when atmospheric absorption is considered. One critical point to consider related to this work is that cross-calibration of sensors must consider the band differences to provide accurate results. The method described in this work considers these band effects.

**Table 1. Band centers for ALI, ASTER, ETM+ and TM**

Band	<i>Band Centers (<math>\mu\text{m}</math>)</i>			
	ALI	ASTER	TM	ETM+
1p	0.443	-	-	-
1	0.483	0.554	0.485	0.482
2	0.565	0.661	0.560	0.565
3	0.660	0.807	0.660	0.660
4	0.790	1.652	0.830	0.825
4p	0.868	-	-	-
5p	1.250	-	-	-
5	1.650	2.164	1.650	1.650
6	-	2.204	-	-
7	2.215	2.259	2.215	2.220
8	-	2.329	-	-
9	-	2.394	-	-

There are several key platform parameters that are important for this work. Landsat-7 ETM+ and Terra ASTER are separated by only 30 minutes in their orbits. ALI originally was in an orbit within minutes of ETM+ but the platform has been allowed to drift since 2005 and no longer coincides with ETM+ in either day or time. Landsat-5 is in an orbit that is eight days out of phase from Landsat-7 and Terra. One interesting feature of the Landsat orbit is an overpass of one sensor at Ivanpah Playa follows an overpass of the other platform at Railroad Valley on the preceding day. This does not allow cross calibration, but it does mean that several data sets collected for TM have corresponding

data sets for ETM+ that occur close in time to one another and were collected by the same group of personnel using the same equipment. All of the data used in this work has a view angle for the sensors that is <8 degrees from nadir.

### Reflectance-based Results

The same basic method is applied to all four sensors in this work. Atmospheric measurements are made and processed in the same fashion but the accuracy of an individual data set's atmospheric characterization will vary based on the accuracy of the calibration of the solar radiometers used in the retrievals. The surface reflectance retrieval relies on transporting a spectroradiometer across a selected area. The approach adopted for the pushbroom sensors collects 8 samples within a 20-m by 20-m area. A total of 60 of these areas are sampled in a 4 by 15 grid with the longer edge oriented in the cross-track direction of the platform. The reflectance sampling for the whiskbroom sensors consists of 10 samples within a 30-m by 30-m area. A total of 64 areas are sampled in a 4 by 16 grid with the longer edge oriented in the along-track direction of the sensor.

The radiative transfer code is identical for all four sensors and the input parameters are identical in form as well. Spectral differences between sensors are taken into account by computing the at-sensor radiance via the MODTRAN radiative transfer code at 1-nm intervals from 350-2500 nm. The hyperspectral, predicted radiances are band-averaged using the appropriate spectral response of a given band to determine the in-band spectral radiance.

Figure 1 shows the results of the reflectance-based method for ETM+ for all dates after 2003. Calibration coefficients are shown for all six of the reflective bands (1-5, and 7). The solid lines for each band are the average calibration coefficient for all dates. The dashed lines are the preflight calibration coefficients. Error bars for each point are the assumed uncertainty for the reflectance-based approach which is currently 2.5% absolute. Key points from the figures is that there is generally good agreement with the preflight calibration on average, there tends to be scatter to the results, and there are no definite trends in the data with time. The scatter of the data points by date is one of the main issues with the reflectance-based approach and the cross-calibration method described later in the paper attempts to reduce these effects. Work is currently underway to understand the causes of the scatter, but no single cause has been found to date.

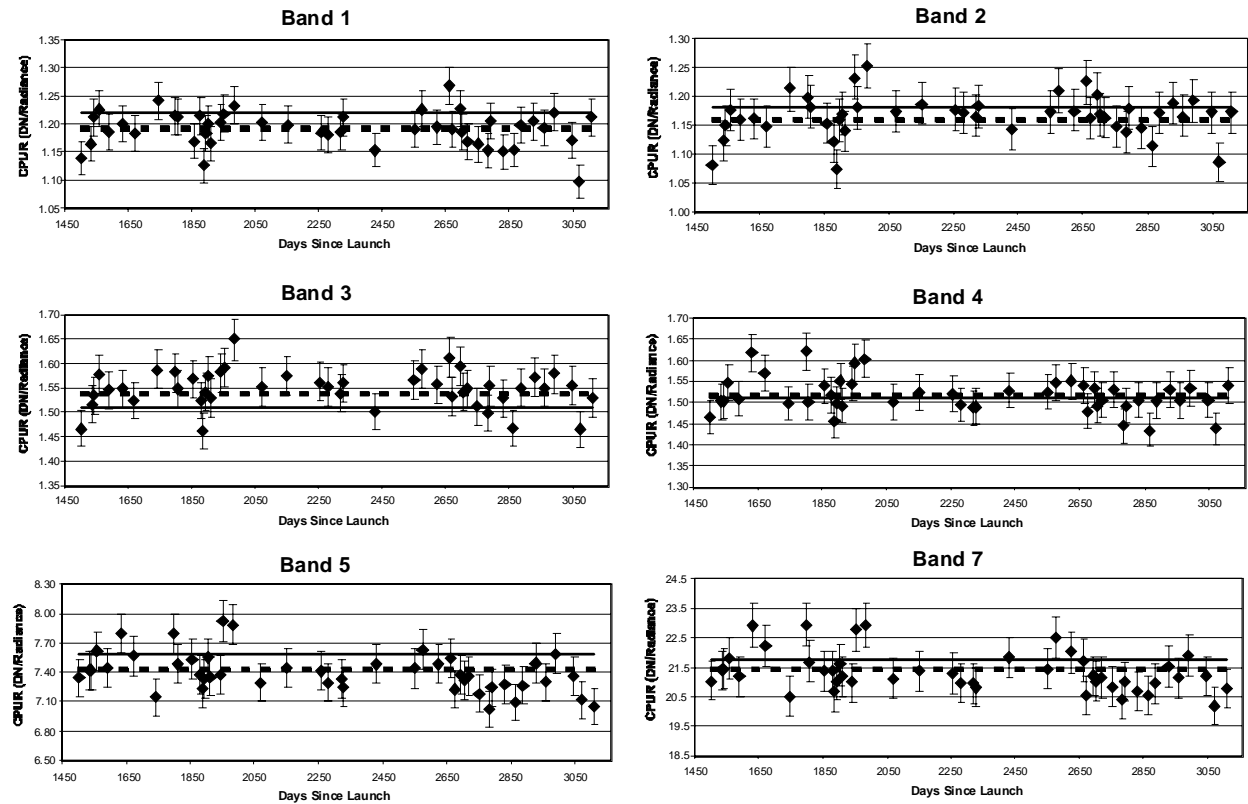
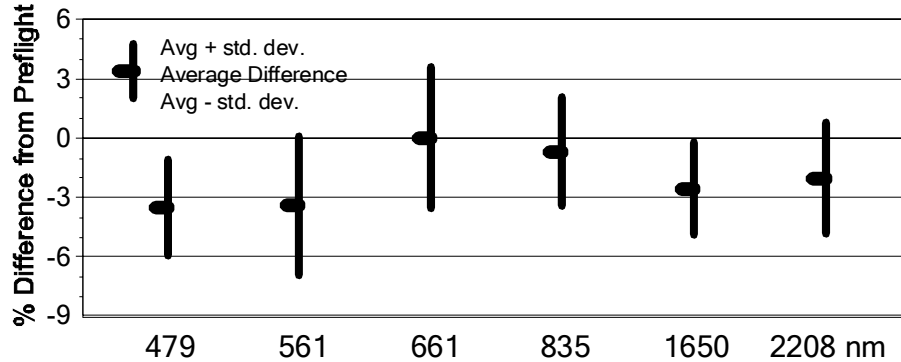


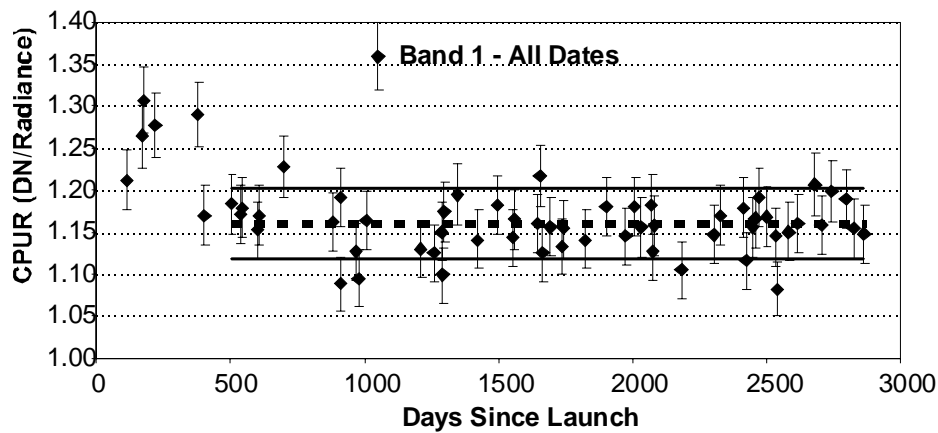
Figure 1. Reflectance-based results for ETM+ for all dates after 2003 collected at all test sites.

Figure 2 summarizes the temporal data for Landsat-7 ETM+ results from 59 data sets collected between 1999 and 2005. The figure shows the average percent difference between the predicted calibration coefficient for ETM+ based on the reflectance-based results of the RSG. The standard deviation for all bands is less than +/-3% and less than 2% for several bands. This standard deviation can be viewed as a proxy for the precision of the reflectance-based retrieval and implies that the precision is better than 3%.



**Figure 2.** Reflectance-based results for ETM+ based on 59 data sets collected at all test sites.

For comparison, results for Band 1 from ASTER are given in Figure 3. The results later in the lifetime of ASTER are similar in scatter to those from ETM+. The dashed line in this case represents the average of the points after day 500 and the solid lines are +/- one standard deviation from the average. One difference between the ASTER and ETM+ results is that the derived calibration coefficients in counts per unit radiance (CPUR) are significantly larger than the average early in mission. Data from other sources verify that there has been degradation in the response for the VNIR bands of ASTER. In addition, the ASTER data sets are collected on the same date and same location as the ETM+ data sets. The ETM+ results do not show a similar temporal trend, thus implying that the reflectance-based method is not the cause of the effect seen in the graph. The temporal frequency of the data and the precision of the reflectance-based approach prevent trending of the data with any statistical confidence, but the change in coefficients is readily apparent.



**Figure 3.** Reflectance-based results for ASTER Band 1.

Similar graphs can be produced for ALI, and TM as well. The results of the work for all four sensors show that the reflectance-based method is useful in detecting sensor degradation and anomalies. This is evident in the results for ASTER which shows degradation in the VNIR bands, an optical crosstalk effect in the shortwave infrared, and the change in offset due to a cooler problem for the SWIR bands. Trending of degradation is difficult due to the variable nature of the results as seen in Figure 3. The next section demonstrates that combining the results in the figures above allows the sensors to be cross-calibrated using the reflectance-based method as the transfer standard.

## INTERCOMPARISON RESULTS

The results shown in Figures 1-3 display a range of possible methods for evaluating the radiometric calibration of a sensor using the reflectance-based method. The ETM+ results, for example are shown as both a computed calibration coefficient and as a percent difference from the preflight calibration. Another approach includes computing percent difference in reported radiance by the given sensor to the predicted radiance from the reflectance-based results. Applying the approach shown for the ETM+ and ASTER sensors in Figures 1 and 3 provide data sets that are internally consistent between the sensors. That is, using a calibration coefficient determined based on sensor output and vicarious prediction provides a set of coefficients that cross-calibrates the sensors using the vicarious results as a transfer standard.

An alternative approach is shown in Figure 4 in which the goal would be to develop a set of calibration coefficients for a single sensor that allows it to compare well with a different sensor. Consider the case where a user already has a set of ETM+ data and they wish to include ALI and ASTER data in the study. Comparisons of the ALI and ASTER results against the reflectance-based method shows Band 1 of ASTER disagrees by 6.8% with ETM+ band 2 and Band 2 of ALI by X.X%. The user should then adjust all of their ASTER Band 1 data by 6.8% and similarly for ALI Band 2.

Such an approach is usually needed when similar bands are being compared, but the approach becomes more difficult to apply when the desire is to use all of the ASTER bands in the study and the hope is to have a consistent ETM+/ASTER data set. In that case, the SWIR bands 7-9 could be corrected to agree with ETM+ band 7, but this may not necessarily be the best approach. The recommended method in such a case would be to correct both data sets relative to the 0% line in both graphs.

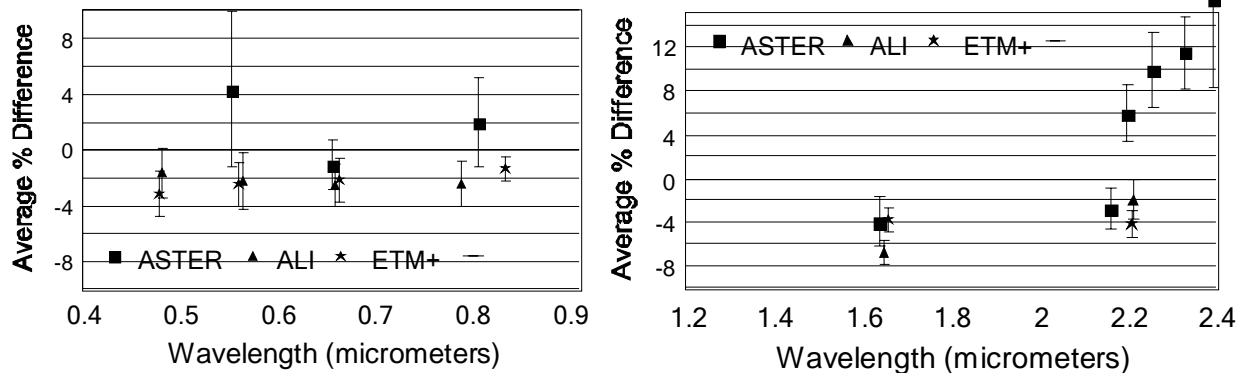


**Figure 4.** Cross-comparison results between ASTER and ETM+ allowing the determination of a cross-calibration between the two sensors. Data are based on Level 1B data from ASTER processed with post-2006 calibration

## LANDSAT INTERCOMPARISON PRECISION IMPROVEMENT

The approach above does not readily lend itself to cases where there are changes in the calibration of the sensor with time. The solution to these situations is to use whatever methods are needed to determine the temporal changes in the radiometric calibration and then use the cross calibration approach to anchor that radiometric calibration curve. The TM sensor is a good example of a system that has suffered significant degradation with time. TM is also a good test bed for this approach since a cross-calibration with TM and ETM+ using typical methods is not trivial due to the eight-day difference in orbit. In addition, the stability of TM and ETM+ in recent years allows for an evaluation of the limits of the precision of this approach to be evaluated.

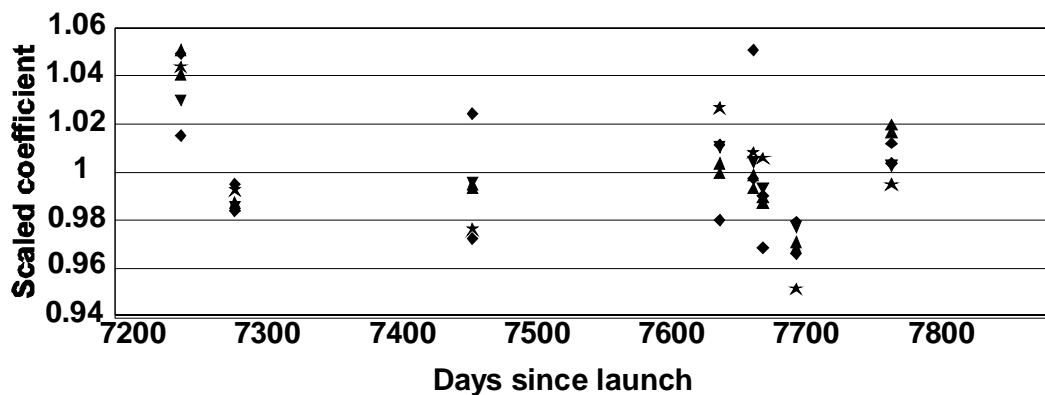
The first step in the Landsat-5 TM calibration determination is to find the best dates from the reflectance-based method from RSG at all sites. The period 2004 to 2005 was chosen as the cross-calibration period since ground data collected during that period showed good agreement between the RSG results and the preflight calibration of ETM+. Furthermore, degradation in TM and ETM+ is minimal for this period allowing averages to be determined across the entire period permitting a sufficient number of dates of data to evaluate accuracy and precision. Later dates are not included due to the issues with the Landsat-5 platform beginning in December 2005 causing complications in scheduling field collections and a lack of ground data.

Table 2 shows eight Landsat-5 TM dates in 2004 and 2005 for which the RSG has results. An additional nine dates of collection were attempted during the period with poor weather or poor surface conditions/snow preventing data collections in January, February, March, and June 2004, and January, February, March, April, and November 2005. The results from the eight successful collections currently processed are included in Table 2.

**Table 2. TM Results used in determination of cross-calibration parameters for ETM+**

Date	DSL	Site	Band 1	Band 2	Band 3	Band 4	Band 5	Band 7
13-May-04	7249	RRV	1.237	0.644	0.916	1.102	7.930	14.980
23-Jun-04	7290	Ivan.	1.224	0.651	0.908	1.095	7.922	14.863
16-Dec-04	7466	Ivan.	1.176	0.639	0.906	1.096	8.180	14.435
17-Jun-05	7649	RRV	1.185	0.642	0.915	1.113	8.073	15.185
12-Jul-05	7674	Ivan.	1.271	0.638	0.911	1.106	7.965	14.905
19-Jul-05	7681	RRV	1.171	0.634	0.902	1.094	7.906	14.876
13-Aug-05	7706	Ivan.	1.184	0.622	0.885	1.076	7.712	14.074
23-Oct-05	7777	RRV	1.213	0.655	0.927	1.104	8.081	14.718
Average	---	---	1.208	0.641	0.909	1.098	7.971	14.755
Std. Dev.	---	---	0.035	0.010	0.012	0.011	0.142	0.349
% Std. Dev.	---	---	2.9	1.6	1.4	1.0	1.8	2.4

The results show relatively small standard deviations in the average indicating that the data are of good quality. The results are shown graphically Figure VVV where each of the individual bands and dates have been scaled relative to the average allowing easier comparisons between bands. Features of note are that the scatter of the points varies from day to day and it appears that small, correlated biases appear in the data sets from day to day.



**Figure 5.** TM reflectance-based results corresponding to Table 2. Different symbols represent different bands and all results are scaled relative to the average shown for each band in Table 2.

The goal of this work is to provide the Landsat-5 TM calibration with the highest confidence, thus it was decided to use only the “best” days of reflectance-based results for the period. Many options for selecting the dates are available ranging from selecting those dates with the lowest atmospheric optical depths, the highest surface reflectance, a specific aerosol size distribution, a certain season, etc. The process applied here selects those dates for which scaled calibration coefficients showed the least spectral scatter. No preference is given in terms of how well the average on a given date agrees with the overall average for a given band only the scatter between bands.

The standard deviations of the averages for each of the eight dates ranged from 0.9 to 2.1%. An arbitrary cut off of 1% was selected since this was both a natural break point in the data set as well as leaving four days of data to be used. This number of dates is important as statistical analysis of the expected accuracies shows that four data sets are sufficient to estimate the calibration coefficient to within 2.5% at a 95% confidence interval (Thome et al., 2005a). The dates omitted from further analysis and their standard deviations are 16-Dec-04 (1.9%), 17-Jun-05 (1.6%), 12-Jul-05 (2.1%), and 19-Jul-05 (1.3%).

It is of interest to understand the causes of the larger scatter on certain dates, but the cause is not critical for this analysis. Likely sources of band-to-band scatter on a given date are spectral-spatial variations in the surface reflectance, errors in knowledge of atmospheric conditions including the use of an incorrect aerosol model, processing errors, and larger than normal noise in the reflectance measurements. Future work will investigate the causes of the scatter, but the end result here is that four days remained. The average values for the calibration coefficients for the full data set and the four selected data points changed by only a small amount. The largest differences occur for bands 5 and 7 which both decreased by 0.7%. One disappointing feature was that the standard deviations of the averages increase in all bands except band 1. The increases are small, however, and considering the fact that number of points in the standard deviation decreased by a factor of two is encouraging.

Additional examination of Figure 5 indicates that further improvement in precision in the derived calibration coefficients is feasible by noting that all bands have a similar bias from the average for a given date. Such a correlated effect implies that the reflectance-based results on a given date have a consistent bias. The most likely cause is a bias caused by the surface reflectance measurements since the spectral effect is small. The last step in the calculations is to scale each of the data points by an amount determined from the bias in a selected band from its average. The average of Band 3 remained the same between the eight- and four-date data sets and was selected as the reference band. Ratios of the difference between the calibration coefficient for band 3 on a given date to the average are computed and used to scale all other coefficients. The scaled coefficients are shown in the Table 3

The results from the eight successful collections currently processed are included in Table 2.

**Table 3. Selected four data sets of TM results scaled relative to Band 3**

Date	DSL	Site	Band 1	Band 2	Band 3	Band 4	Band 5	Band 7
13-May-04	7249	RRV	1.228	0.639	0.909	1.094	7.869	14.866
23-Jun-04	7290	Ivan.	1.225	0.652	0.909	1.096	7.931	14.879
13-Aug-05	7706	Ivan.	1.216	0.639	0.909	1.105	7.921	14.456
23-Oct-05	7777	RRV	1.189	0.642	0.909	1.083	7.924	14.432
Average	---	---	1.215	0.643	0.909	1.094	7.911	14.658
Std. Dev.	---	---	0.017	0.006	---	0.009	0.028	0.248
% Std. Dev.	---	---	1.4	0.9	---	0.9	0.4	1.7

The results for Band 3 are the same it is scaled relative to its own average. The results for other bands show effectively no change in the average with dramatic improvements in the standard deviation. The normalization process removes biases most likely caused by biases in the reflectance characterization. It is most likely that atmospheric bias effects have been removed in the scatter-screening process. The results shown here are believed to be the best estimates for the absolute radiometric calibration coefficients for Landsat-5 TM. Note that the average calibration coefficients do not change significantly from the full data set to the re-normalized and scaled coefficients. What has changed dramatically is the standard deviation of the data sets.

A similar process has been applied to ETM+ data. Key differences are that a total of 17 data sets were available for ETM+ for the 2004-2005 period. Using a 1% standard deviation screening for scatter left seven dates in the period giving the averages and standard deviations shown in Table 4, and scaling relative to band 3 gives the last two rows of the table. Additionally, results after scaling relative to Band 4 have been included for reference.

Use of the scatter-screened, band 3-normalized results for both TM and ETM+ give results consistent with each other to better than 2%. The users of ETM+ data, however, will most likely use preflight calibration information for ETM+. It makes sense then, to normalize the TM calibration coefficients relative to the ETM+ preflight calibration. This is done by multiplying the TM coefficients by the ratio of the ETM+ preflight calibration to the scatter-screened, band-normalized ETM+ results. This gives the final, best estimate values for the TM calibration coefficients that will produce ETM+ equivalent radiances based on preflight calibration of ETM+. The values are shown in Table 5

**Table 4. Results of full 17 and selected seven ETM+ dates from 2004-2005 for cross-calibration**

Date		Band 1	Band 2	Band 3	Band 4	Band 5	Band 7
Average	Full data 2004-2005 data set	1.191	1.174	1.567	1.529	7.451	21.243
%Std. Dev.		2.2	4.1	3.7	3.7	4.2	6.2
Average	Scatter-screened seven dates	1.185	1.167	1.554	1.509	7.388	21.187
%Std. Dev.		1.0	1.3	1.2	1.5	1.2	1.1
Average	Band 3 normalized	1.185	1.167	1.554	1.509	7.388	21.187
%Std. Dev.		0.6	0.7	---	0.8	0.8	0.9
Average	Band 4 normalized	1.186	1.167	1.554	1.509	7.389	21.188
%Std. Dev.		1.0	1.4	0.7	---	0.5	0.6

**Table 5. Final TM calibration coefficients based on cross-calibration to ETM+ using reflectance-based results**

	Band 1	Band 2	Band 3	Band 4	Band 5	Band 7
L5 TM	1.250	0.650	0.884	1.095	8.127	15.048

## CONCLUSIONS

The methods described above describe an approach that permits the cross-calibration of sensors without the need for coincident views and sites. The method does require in situ measurements limiting its application to those test sites for which ground data are feasible. Normally, the use of ground-based measurements creates a set of data that suffers from large scatter in the results. Scaling of the results based on day-to-day correlations and selecting only those dates for which spectral variation in the data are minimized results in a precision better than 2% in all bands and approaching 1% in several spectral bands.

The key conclusion from this work is that it is feasible to cross-calibrate sensors at a 1-2% level even in situations when there are gaps in the data sets. Results will be improved if the ground measurements are made in a consistent fashion but the ultimate goal should be to make measurements in a traceable fashion with high precision. The ultimate outcome is that a long-term Landsat series of data should be feasible even in the unfortunate case that ETM+ or TM cease operation prior to the launch of the Operational Land Imager.

## REFERENCES

- Butler, J.J. and R. A. Barnes, "Calibration strategy for the Earth Observing System (EOS)-AM1 platform, 1998, *IEEE Trans. On Geoscience and Remote Sensing*, 36:1056-1061.
- Cabot, F. O. Hogolle, H. Consnefroy, and X. Briottet, 1999, "Inter-calibration using desertic sites as a reference target," *IEEE -0-7803-4403*.
- Goward, S. N., J. G. Masek, D. L. Williams, J. R. Irons, R. J. Thompson, 2001, "The Landsat-7 mission: Terrestrial research and applications for the 21st century," *Remote Sens. Environ* 78:3-12.
- Kaufman, Y. J. and B. N. Holben, 1993, "Calibration of the AVHRR visible and near-IR bands by atmospheric scattering, ocean glint, and desert reflection," *Intl. J. Remote Sensing*, 14, :21-52.
- Kaufman, Y. J., D. D. Herring, K. J. Ranson, and G. J. Collatz, 1998, "Earth Observing System AM1 mission to

- Earth," *IEEE Trans. On Geoscience and Remote Sensing*, 36 :1045-1055.
- Lencioni, D. E., C. J. Digenis, W. E. Bicknell, D. R. Hearn, and J. A. Mendenhall, 1999 "Design and Performance of the EO-1 Advanced Land Imager," *Proc. of SPIE #3870*.
- Robichaud, J., J. J. Guregian, and M. Schwalm, 2003, "SiC optics for Earth observing applications," *Proc. SPIE # 5151*, Vol. 5151.
- Slater, P. N., S. F. Biggar, K. J. Thome, D. I. Gellman, and P. R. Spyak, 1996, "Vicarious radiometric calibrations of EOS sensors," *J. of Atmospheric and Oceanic Technology*, 13:349-359.
- Slater, P. N., S. F. Biggar, R. G. Holm, R. D. Jackson, Y. Mao, M. S. Moran, J. M. Palmer, and B. Yuan, 1987, "Reflectance- and radiance-based methods for the in-flight absolute calibration of multispectral sensors," *Rem. Sens. Env.*, Vol. 22:11-37.
- Thome, K. J., "Absolute radiometric calibration of Landsat-7 ETM+ using the reflectance-based method," 2001, *Remote Sensing of Environment*, 78:27-38
- Thome, K., B. Markham, J. Barker, P. Slater, and S. Biggar. 1997. "Radiometric calibration of Landsat," *Photogramm. Eng. and Remote Sensing*. 63: 853-858.
- Thome, K, C. Catrall, J. D'Amico, and J. Geis, 2005a, "Ground-reference calibration results for Landsat-7 ETM+", *Proc. SPIE Conf. #5882*.
- Thome, K. J., D. I. Gellman, R. J. Parada, S. F. Biggar, P. N. Slater, and M. S. Moran, 1993, "In-flight radiometric calibration of Landsat-5 Thematic Mapper from 1984 to present," *Proc. of SPIE*, Vol. 1938.
- Thome, K. J., D. L. Helder, D. Aaron, and J. D. Dewald, "Landsat-5 TM and Landsat-7 ETM+ absolute radiometric calibration using the reflectance-based method," *IEEE Trans. On Geosciences and Remote Sensing*, 42:2777-2785.
- Thome, K. J. Czapla-Myers, S. F. Biggar, 2003 "Vicarious calibration of Aqua and Terra MODIS," *Proc. SPIE Conf. #5151*, San Diego, Calif.
- Thome, K., J. D'Amico, C. Hugon, 2006, "Intercomparison of Terra ASTER, MISR, and MODIS, and Landsat-7 ETM+, *Proc. IGARSS*, Denver, Colo.
- Thome, K., J. Geis, C. Catrall 2005b, "Comparison of ground-reference calibration results for Landsat-7 ETM+ for large and small test sites", *Proc. SPIE Conf. #5882*.
- Vermote, E. and Y. Kaufman, 1995, "Absolute calibration of AVHRR visible and near-infrared channels using ocean and cloud views." *Intl. J. Remote Sensing*, 16:2317-2340.
- Vermote, E., R. P. Santer, P. Y. Deschamps, and M. Herman. 1992 "In-flight calibration of large field of view sensors at short wavelengths using Rayleigh scattering." *Int. J. of Rem. Sens. Vol. 13*:3409-3429.
- Yamaguchi, Y., A. Kahle, H. Tsu, T. Kawakami, and M. Pniel, 1998, "Overview of Advanced Spaceborne Thermal Emission and Reflection Radiometer (ASTER)," *IEEE Trans. On Geoscience and Remote Sensing*, 36.